Available online at www.sciencedirect.com
ScienceDirect
Atmospheric Environment 41 (2007) 1188–1199
ATMOSPHERIC ENVIRONMENT
www.elsevier.com/locate/atmosenv

Geraniol (2,6-dimethyl-2,6-octadien-8-ol) reactions with ozone and OH radical: Rate constants and gas-phase products

Crystal D. Forester, Jason E. Ham, J.R. Wells*

Exposure Assessment Branch, Health Effects Laboratory Division, National Institute for Occupational Safety and Health, 1095 Willowdale Road, Morgantown, WV 26505, USA

Received 29 August 2006; received in revised form 15 September 2006; accepted 22 September 2006

Abstract

The bimolecular rate constants, $k_{OH+geraniol}$, $(231 \pm 58) \times 10^{-12}$ cm^3 molecule^{-1} s^{-1} and $k_{O_3+geraniol}$, $(9.3 \pm 2.3) \times 10^{-16}$ cm^3 molecule^{-1} s^{-1}, were measured using the relative rate technique for the reaction of the hydroxyl radical (OH) and ozone (O_3) with 2,6-dimethyl-2,6-octadien-8-ol (geraniol) at (297 ± 3) K and 1 atmosphere total pressure. To more clearly define part of geraniol's indoor environment degradation mechanism, the products of the geraniol + OH and geraniol + O_3 reactions were also investigated. The identified geraniol + OH and geraniol + O_3 reaction products were: acetone, hydroxyacetaldehyde (glycolaldehyde, HC(=O)CH$_2$OH), ethanedial (glyoxal, HC(=O)C(=O)H), and 2-oxopropanal (methylglyoxal, CH$_3$C(=O)C(=O)H). The use of derivatizing agents O-(2,3,4,5,6-pentafluorobenzyl)hydroxylamine (PFBHA) and N,O-bis(trimethylsilyl) trifluoroacetamide (BSTFA) were used to propose 4-oxopentanal as the other major geraniol + OH and geraniol + O_3 reaction product. The elucidation of this other reaction product was facilitated by mass spectrometry of the derivatized reaction products coupled with plausible geraniol + OH and geraniol + O_3 reaction mechanisms based on previously published volatile organic compound + OH and volatile organic compound + O_3 gas-phase reaction mechanisms.
Published by Elsevier Ltd.

Keywords: Geraniol; 2,6-dimethyl-2,6-octadien-8-ol; Reaction products; Kinetics; Oxygenated organic compounds

1. Introduction

Work-related asthma (WRA) has increasingly become one of the most commonly reported respiratory diseases in the U.S (NIOSH, 2004). The reason for the increases in WRA has been partially attributed to the presence of volatile organic compounds (VOCs) (Dales and Raizenne, 2004; Weisel, 2002; Wieslander et al., 1997; Zhang and Smith, 2003). Experimental evidence has implicated that several initiator species such as ozone (O_3), hydroxyl radical (OH), and nitrate radical (NO_3) are present indoors converting VOCs that are present (i.e. emissions from cleaning products, air fresheners) into other oxygenated organic compounds such as aldehydes and ketones (Sarwar et al., 2002; Weschler, 2001; Weschler and Shields, 1997a, b). In a recent paper by Jarvis et al., chemicals with these carbonyl substructures were associated with the potential to cause WRA (Jarvis

*Corresponding author. Tel.: +1 304 285 6341; fax: +1 304 285 6041.
E-mail address: ozw0@cdc.gov (J.R. Wells).

1352-2310/$ - see front matter Published by Elsevier Ltd.
doi:10.1016/j.atmosenv.2006.09.042

et al., 2005). Before attributing a particular VOC or group of VOCs to the effect of WRA, identification and quantification of organic compounds present in the indoor environment are necessary to determine occupant exposures. Additionally, the mechanisms from which these are emitted or formed must also be understood to provide guidance for structure-based chemical selection. With this knowledge, new compounds may be synthesized that incorporate environmentally and technically beneficial molecular structures. The information gained from the type of research presented here can lead to more beneficial use of these and similar compounds in the future.

Oxygenated organic compounds, such as ethers, alcohols, and esters, are also becoming more prevalent in the indoor environment as they are substituted for other chemicals in consumer products. While several OH + oxygenated organic and O_3 + oxygenated organic bimolecular rate constants are well known, the details of their reaction mechanisms are limited (Atkinson, 1989; Atkinson, 1994). A few recent studies of the products from OH + oxygenated organic reactions have illustrated the complexity of their gas-phase reaction mechanisms (Bradley et al., 2001; Smith et al., 1992, 1995; Veillerot et al., 1996; Wallington et al., 1993; Wells, 2004, 2005; Wells et al., 1996; Wyatt et al., 1999). These investigations are needed to support OH and O_3 reaction mechanism patterns based on chemical structure–reactivity relationships (Boethling and Mackay, 2000).

One such compound of interest is 2,6-dimethyl-2,6-octadien-8-ol (geraniol, Structure 1) a volatile organic alcohol that is a significant component of indoor cleaner emissions and a component of the rose oil scent (Nazaroff and Weschler, 2004).

In the work presented here, the rate constants for the geraniol + OH radical reaction and the geraniol + O_3 reaction have been measured using the relative rate method. Some products of these reactions (geraniol + OH and geraniol + O_3) are also reported. Neither the OH rate constant, nor the respective reaction mechanisms for OH + geraniol have been reported previously. The geraniol + O_3 rate constant and reaction mechanisms were previously studied by Nunes et al. (Nunes et al., 2005) and those results will be compared with the results of this study.

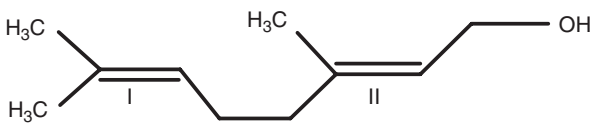

Structure 1. 2,6-dimethyl-2,6-octadien-8-ol.

2. Experimental methods

2.1. Apparatus and materials

Experiments to measure the gas-phase rate constant of the OH + 2,6-dimethyl-2,6-octadien-8-ol (geraniol, Structure 1) reaction were conducted with a previously described apparatus (Atkinson et al., 1981; Orji and Stone, 1992; Veillerot et al., 1996; Williams et al., 1993). A brief description is provided here. Reactants were introduced and samples were withdrawn through a 6.4-mm Swagelok fitting attached to a 80–110 L Teflon film chamber. Compressed air from the National Institute for Occupational Safety and Health (NIOSH) facility was passed through anhydrous $CaSO_4$ (Drierite, Xenia, OH) and molecular sieves (Drierite, Xenia, OH) to remove both moisture and organic contaminants. This dry compressed air was added as a diluent to the reaction chambers and measured with a 0–100 L min^{-1} mass flow controller (MKS, Andover, MA). Analysis of this treated compressed air by gas chromatography/mass spectrometry revealed that if contaminants were present they would be below the part per trillion range. The filler system was equipped with a syringe injection port facilitating the introduction of both liquid and gaseous reactants into the chambers with the flowing air stream. All reactant mixtures and calibration standards were generated by this system. Irradiations were carried out in a light-tight chamber housing surrounding 5-mil FEP Teflon-film chambers (80–110 L), which contained the following mix of lamps: six Philips TL40W/03; one GE F40BL; two QPANEL (Cleveland, OH) UV351 and seven QPANEL UV340. This lamp mixture approximates solar radiation from 300 to 450 nm.

All reaction kinetic samples were quantitatively monitored using an Agilent (Palo Alto, CA) 6890 gas chromatograph with a 5973 mass selective detector (GC/MS) and Agilent ChemStation software. Gas samples were cryogenically collected employing an Entech 7100 (Simi Valley, CA) sampling system utilizing the following trap and temperature parameters: 50 mL of chamber contents were collected onto Trap 1 (packed silanized glass beads) at −150 °C. After sample collection

Trap 1 was heated to 230 °C and the sample transferred under a flow of ultra high purity helium (UHP He) onto Trap 2 (packed silanized glass beads) cooled to −30 °C. Trap 2 was then heated to 180 °C and the sample transferred under a UHP He flow onto Trap 3, a silanized 0.53 mm i.d. tube cooled to −160 °C which was subsequently heated to 220 °C to inject the sample onto an Rtx-VRX (Restek, Bellefonte, PA) GC column (0.25 mm i.d., 30-m long, 1.4 μm film thickness). These series of cryogenic trap manipulations reduced the background water level, ensured consistency of replicate samples, and improved the chromatograph peak shapes. The GC temperature program used was: initial temperature of 45 °C held for 8 min after sample injection then increased 10 °C min^{-1} to 220 °C and held for 4 min. The Agilent 5973 mass selective detector was tuned using perfluorotributylamine (FC-43). Full-scan electron impact (EI) ionization spectra were collected from m/z 35 to 650. Preliminary compound identifications from the Agilent 6890/5973 GC/MS data sets were made by searching the NIST 98 Mass Spectral Library.

Identification of reaction products was made using O-(2,3,4,5,6-pentafluorobenzyl)hydroxylamine (PFBHA) to derivatize carbonyl products, while alcohol and carboxylic acid products were derivatized using PFBHA and N,O-bis(trimethylsilyl)trifluoroacetamide (BSTFA) (Fick et al., 2003; Yu et al., 1998). Experimental methods for reaction product identification were similar to methods used for kinetic experiments, except the reference compound was excluded from the reaction mixture. An additional port was added to the Teflon chamber to facilitate the injection of ozone.

Derivatized reaction products were analyzed using a Varian (Palo Alto, CA) 3800/Saturn 2000 GC/MS system operated in both the EI and CI modes (Yu et al., 1998). Compound separation was achieved by a J&W Scientific (Folsom, CA) DB-5MS (0.32 mm i.d., 30-m long, 1 μm film thickness) column and the following GC oven parameters: 60 °C for 1 min then 20 °C min^{-1} to 170 °C, then 3 °C min^{-1} to 280 °C and held for 5 min.

Samples were injected in the splitless mode, and the GC injector was returned to split mode 1 min after sample injection, with the following injector temperature parameters: 60 °C for 1 min then 180 °C min^{-1} to 250 °C and held to the end of the chromatographic run (Yu et al., 1998). The Saturn 2000 ion trap mass spectrometer was tuned using FC-43. Full-scan EI ionization spectra were collected from m/z 40 to 650. Acetonitrile was the chemical ionization reagent used for all CI spectra. When possible, commercially available samples of the identified products were derivatized and subsequently analyzed to verify matching ion spectra and chromatographic retention times.

Hydroxyl radicals, which are among the primary oxidizing radicals in the indoor environment (Sarwar et al., 2002; Sexton et al., 2004; Weschler and Shields, 1996; Weschler and Shields, 1997a, b), were generated from the photolysis of methyl nitrite (CH_3ONO) in the presence of nitric oxide (NO) in air (Atkinson et al., 1981). CH_3ONO was prepared in gram quantities using the method of Taylor et al. (1980) and stored in a lecture bottle at room temperature. The CH_3ONO purity (>95%) was verified by GC/MS. Ozone was produced by photolyzing air with a mercury pen lamp in a separate Teflon chamber. Aliquots of this O_3/air mixture were added to the Teflon reaction chamber using a gas-tight syringe.

All compounds were used as received and had the following purities: from Sigma-Aldrich (Milwaukee, WI): cyclohexane (99.9%), hexane (99%), limonene (99%), geraniol (98%), cis-cyclooctene (95%), myrcene (90%), acetonitrile (99.93%), BSTFA (99 + %), PFBHA hydrochloride (98 + %), glycolaldehyde dimer (98%), glyoxal (40% in water) and methyl glyoxal (40% in water); from Fisher Scientific (Fairlawn, NJ): methanol (99%); from Spectrum Analytical (New Brunswick, NJ): methylene chloride (99.5%). Nitric oxide (99 + % pure) was obtained as a 4942 ppm mixture in nitrogen from Butler Gases (Morrisville, PA). Helium (UHP grade), the carrier gas, was supplied by Amerigas (Sabraton, WV) and used as received. Experiments were carried out at (297 ± 3) K and 1 atm pressure.

2.2. Experimental procedures

The experimental procedures for determining the geraniol + OH and geraniol + O_3 reaction kinetics were similar to those described previously (Bradley et al., 2001; Wells, 2004; Wyatt et al., 1999).

$$\text{Geraniol} + \text{OH or } O_3 \xrightarrow{k_{\text{OH+Geraniol}} \text{ or } k_{O_3+\text{Geraniol}}} \text{Products} \quad (1)$$

$$\text{Reference} + \text{OH or } O_3 \xrightarrow{k_{\text{Ref}}} \text{Products} \quad (2)$$

The rate equations for reactions 1 and 2 are combined and integrated, resulting in the following

equation:

$$\ln\left(\frac{[\text{Geraniol}]_0}{[\text{Geraniol}]_t}\right) = \frac{k_{\text{OH+Geraniol}} \text{ or } k_{\text{O}_3\text{+Geraniol}}}{k_{\text{Ref}}} \times \ln\left(\frac{[\text{Ref}]_0}{[\text{Ref}]_t}\right). \quad (3)$$

If reaction with OH or O_3 is the only removal mechanism for geraniol and reference, a plot of $\ln([\text{geraniol}]_0/[\text{geraniol}]_t)$ versus $\ln([\text{Ref}]_0/[\text{Ref}]_t)$ yields a straight line with an intercept of zero. Multiplying the slope of this linear plot by k_{Ref} yields $k_{\text{OH + geraniol}}$ (Fig. 1) or $k_{\text{O}_3\text{+geraniol}}$ (Fig. 2). The OH rate constant experiments for geraniol employed the use of two reference compounds: limonene and myrcene. The use of two different reference compounds with different OH rate constants or O_3 rate constants aids to ensure the accuracy of the geraniol + OH rate constant or geraniol + O_3 rate constant and demonstrates that other reactions are not removing geraniol.

For the geraniol + OH kinetic experiments the typical concentrations of the pertinent species in the 80–110 L Teflon chamber were 0.5–0.9 ppm (1.3–2.2×10^{13} molecule cm^{-3}) geraniol, 0.1–0.3 ppm (1.7–6.9×10^{12} molecule cm^{-3}) reference, 10 ppm (23×10^{13} molecule cm^{-3}) CH_3ONO, and 0.6 ppm (1.4×10^{13} molecule cm^{-3}) NO in air. The gas-phase mixtures were allowed to reach equilibrium before initial species concentration ($[X]_0$) samples were collected. Typically, three photolysis intervals of 3–5 s each were used on the reaction mixture for a combined total photolysis time of approximately 9–15 s. The total ion chromatogram (TIC) from the Agilent 5973 mass selective detector was used to determine geraniol and reference concentrations.

For the geraniol + O_3 kinetic experiments the typical concentrations of the pertinent species in the 80–110 L Teflon chamber were 0.5–0.9 ppm (1.3–2.2×10^{13} molecule cm^{-3}) geraniol, 0.1–0.3 ppm ($2.2–6.9 \times 10^{12}$ molecule cm^{-3}) reference. Cyclohexane (297 ppm, 7.3×10^{15} molecules) was added to the geraniol + O_3 reaction product experiments to scavenge OH radicals (Paulson et al., 1999). The gas-phase mixtures were allowed to reach equilibrium before initial species concentration ($[X]_0$) samples were collected. Typically, three or four injections of ozone resulting in an O_3 concentration of 20–40 ppb in the reaction chamber were used. Ozone was injected into the chamber and allowed to reach equilibrium for approximately 45 min before the samples were collected. The ozone concentration was measured using a thermo-electron UV photometric ozone analyzer Model 49C. The injections of ozone took place over a 2 day period. Samples were collected at the end of the day, the chamber was allowed to sit overnight and samples were collected the following morning. These samples were compared to the previous samples to ensure losses were minimal. The TIC from the Agilent 5973 mass

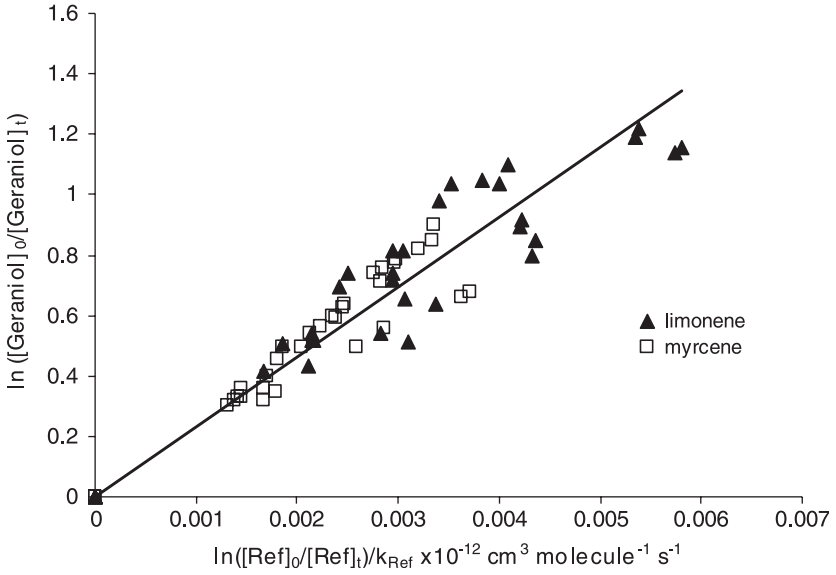

Fig. 1. 2,6-dimethyl-2,6-octadien-8-ol (geraniol) relative rate plot with myrcene (□) and limonene (▲) as reference compounds. The OH + geraniol rate constant, $k_{\text{geraniol + OH}}$, measured is $(231 \pm 4) \times 10^{-12}$ cm^3 $molecule^{-1}$ s^{-1}.

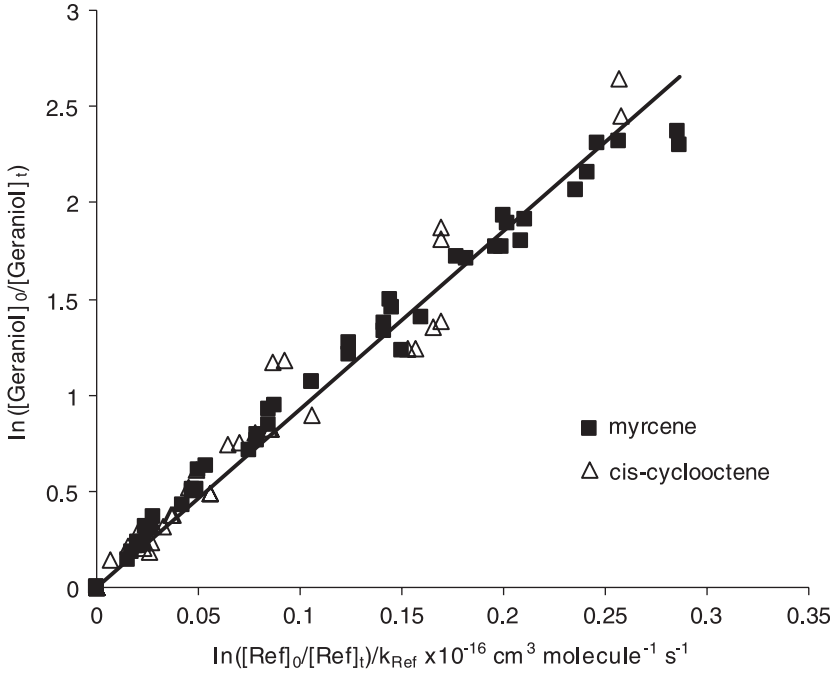

Fig. 2. 2,6-dimethyl-2,6-octadien-8-ol (geraniol) relative rate plot with myrcene (■) and cis-cyclooctene (△) as reference compounds. The O_3 + geraniol rate constant, $k_{\text{geraniol}+O_3}$, measured is $(9.3 \pm 0.10) \times 10^{-16}\,\text{cm}^3\,\text{molecule}^{-1}\,\text{s}^{-1}$.

selective detector was used to determine geraniol and reference concentrations.

To determine possible chromatographic interferences from reference + OH reaction products, both geraniol and the reference compounds were reacted with the OH radical in separate experiments and analyzed as described previously (Wells, 2004). No chromatographic interferences were observed. All measurements were duplicated. A relative standard deviation (the data set standard deviation divided by the data set average) of approximately 3.4% was achieved with the described sampling methods utilizing the Agilent 6890/5973 GC/MS system.

Derivatization of the carbonyl reaction products was initiated by flowing 15 to 25 L of chamber contents at $3.8\,\text{L}\,\text{min}^{-1}$ through an impinger containing 3 mL of acetonitrile and 200 μL of 0.02 M PFBHA in acetonitrile to derivatize the carbonyl reaction products to oximes (Yu et al., 1998) with no effort to prevent acetonitrile evaporation during sample collection. The sample was removed from the impinger and allowed to sit for a 24 to 48 h time period in the dark. The reacted solutions were gently blown to dryness with UHP N_2, reconstituted with 100 μL of methanol, and then 1 μL of the reconstituted solution was injected onto the Varian 3800/Saturn 2000 GC/MS system. The derivatization of hydroxy groups (either alcohol or carboxylic acid) was achieved by subsequent addition of 20 μL of commercially available BSTFA to the PFBHA oximes reconstituted with 100 μl of hexane:methylene chloride (1:1). These PFBHA/BSTFA solutions were heated to approximately 60 °C for 45 min to complete the silylation and then 1 μL of the solution was injected into the Varian 3800/Saturn 2000 GC/MS system (Yu et al., 1998).

3. Results

3.1. Geraniol+OH reaction rate constant

The OH rate constant for geraniol (Structure 1) was obtained using the relative rate method described above. The plot of a modified version of Eq. (3) is shown in Fig. 1. The $\ln([\text{Ref}]_0/[\text{Ref}]_t)$ term is divided by the respective reference rate constant (limonene $(164 \pm 41) \times 10^{-12}\,\text{cm}^3\,\text{molecule}^{-1}\,\text{s}^{-1}$ and myrcene $(215 \pm 54) \times 10^{-12}\,\text{cm}^3\,\text{molecule}^{-1}\,\text{s}^{-1}$) (Atkinson, 2003) and multiplied by $10^{-12}\,\text{cm}^3\,\text{molecule}^{-1}\,\text{s}^{-1}$, resulting in a unitless number. This yields a slope that is equal to the OH + geraniol rate constant, $k_{\text{OH}+\text{geraniol}}$, divided by $10^{-12}\,\text{cm}^3\,\text{molecule}^{-1}\,\text{s}^{-1}$. This modification allows for a direct comparison of the two reference

compound/geraniol data sets. The slope of the line shown in Fig. 1 yields an OH bimolecular rate constant, $k_{OH+geraniol}$, of $(231 \pm 4) \times 10^{-12}$ cm^3 $molecule^{-1}$ s^{-1}. The data points at the origin are experimental points because pre-irradiation, $t = 0$, data showed no detectable loss of geraniol or reference. The error in the rate constant stated above is the 95% confidence level from the random uncertainty in the slope. Incorporating the uncertainties associated with the reference rate constants ($\pm 25\%$ for limonene and myrcene) used to derive the geraniol + OH rate constant yields a final value for $k_{OH+geraniol}$, of $(231 \pm 58) \times 10^{-12}$ cm^3 $molecule^{-1}$ s^{-1} (Atkinson, 2003). The geraniol + OH rate constant, $k_{OH+geraniol}$, has not been previously reported. The observed rate constant is comparable to a $k(calc)_{OH+geraniol} = 180 \times 10^{-12}$ cm^3 $molecule^{-1}$ s^{-1}, calculated using the Environmental Protection Agency's rate constant calculation software, AOPWIN v1.91 (US Environmental Protection Agency, 2000).

3.2. Geraniol+O_3 reaction rate constant

The O_3 rate constant for geraniol (Structure 1) was obtained using the relative rate method described above. The plot of a modified version of Eq. (3) is shown in Fig. 2. The $\ln([Ref]_0/[Ref]_t)$ term is divided by the respective reference rate constant (cis-cyclooctene $(3.8 \pm 0.95) \times 10^{-16}$ cm^3 $molecule^{-1}$ s^{-1} and myrcene $(4.7 \pm 1.2) \times 10^{-16}$ cm^3 $molecule^{-1}$ s^{-1}) (Atkinson, 2003) and multiplied by 10^{-16} cm^3 $molecule^{-1}$ s^{-1}, resulting in a unitless number. This yields a slope that is equal to the O_3 + geraniol rate constant, $k_{O_3+geraniol}$, divided by 10^{-16} cm^3 $molecule^{-1}$ s^{-1}. This modification allows for a direct comparison of the two reference compound/geraniol data sets. The slope of the line shown in Fig. 2 yields an O_3 bimolecular rate constant, $k_{O_3+geraniol}$, of $(9.3 \pm 0.10) \times 10^{-16}$ cm^3 $molecule^{-1}$ s^{-1}. The data points at the origin are experimental points because pre-irradiation, $t = 0$, data showed no detectable loss of geraniol or reference. The error in this rate constant is the 95% confidence interval from the random uncertainty in the slope. Incorporating the uncertainties associated with the reference rate constants ($\pm 25\%$ for myrcene and cis-cyclooctene) used to derive the geraniol + O_3 rate constant yields a final value for $k_{O_3+geraniol}$, of $(9.3 \pm 2.3) \times 10^{-16}$ cm^3 $molecule^{-1}$ s^{-1} (Atkinson, 2003). The observed rate constant can be compared with a $k(calc)_{O_3+geraniol} = 8.6 \times 10^{-16}$ cm^3 $molecule^{-1}$ s^{-1}, calculated using the Environmental Protection Agency's rate constant calculation software, AOPWIN v1.91 (US Environmental Protection Agency, 2000) and a rate constant of approximately 4×10^{-16} cm^3 $molecule^{-1}$ s^{-1} determined from results of Nunes et al. (Nunes et al., 2005).

3.3. Geraniol+OH and geraniol+O_3 reaction products

The reaction products observed from the geraniol + OH reaction (hydrogen abstraction or OH addition) and the geraniol + O_3 addition to the carbon–carbon double bond are listed in Table 1. The geraniol + OH and geraniol + O_3 reaction products observed and positively identified using the pure compound for verification by derivatization were: acetone, hydroxyacetaldehyde (glycolaldehyde, $CH(=O)CH_2OH$), ethanedial (glyoxal, $HC(=O)C(=O)H$), and 2-oxopropanal (methylglyoxal, $CH_3C(=O)C(=O)H$). Structures and ions used to identify these compounds are listed in Table 1. Elucidation of the other major reaction product, 4-oxopentanal, was facilitated by mass spectrometry of the derivatized reaction product coupled with plausible geraniol + OH and geraniol + O_3 reaction mechanisms based on previously published volatile organic compound/OH and volatile organic compound + O_3 gas-phase reaction as described below (Atkinson, 1989; Bradley et al., 2001; Smith et al., 1992, 1995; Veillerot et al., 1996; Wallington et al., 1993; Wells, 2004; Wells et al., 1996; Wyatt et al., 1999).

Derivatization of nonsymmetric carbonyls using PFBHA or PFBHA/BSTFA typically resulted in multiple chromatographic peaks due to geometric isomers of the oximes. Identification of multiple peaks of the same oxime compound is relatively simple since the mass spectra for each chromatographic peak of a particular oxime are almost identical. Typically, the PFBHA-derivatized oximes' (generic structure: $F_5C_6CH_2ON=C(R_1)(R_2)$) mass spectra included an ion at m/z 181 ($[CH_2C_6F_5]^+$ fragment) with a large relative intensity (>40%) and a $[PFBHA\ oxime + 181]^+$ ion (due to reactions in the ion trap mass spectrometer) (Yu et al., 1998). In most cases, the m/z 181 ion relative intensity for the chromatographic peaks due to geraniol + OH and geraniol + O_3 reaction product oximes was either the largest or one of the largest in the mass spectrum and was used to

Table 1
Molecular structure of some geraniol + OH and geraniol + O_3 reaction products

Retention time (min)	Name	Molecular weight (amu)	Structure	CI ions observed
7.6	Acetone	58	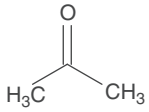	254
10.2 10.5	Hydroxyacetaldehyde (glycolaldehyde)	60	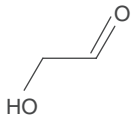	256
24.9 25.2	Ethanedial (glyoxal)	58	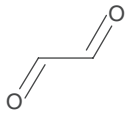	449
26.1	2-oxopropanal (methylglyoxal)	72	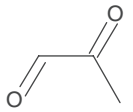	463
30.0 30.3 30.7	4-oxopentanal	100	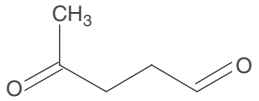	491

generate selected ion chromatograms (Yu et al., 1998). The mass spectra of compounds that were additionally derivatized with BSTFA contained *m/z* 73 ions from the $[Si(CH_3)_3]^+$ fragments (Yu et al., 1998). The product data are described below.

The following chronological chromatographic retention time results and mass spectra data were observed utilizing PFBHA or PFBHA/BSTFA derivatization and the Varian 3800/Saturn 2000 GC/MS system. The reaction products' chromatographic peak areas were a function of the initial geraniol concentration and were observed only after OH initiation of geraniol/methanol/methyl nitrite/NO/air mixtures or addition of O_3 to geraniol/methanol/air. Derivatization experiments performed in the absence of geraniol, but in the presence of all other chemicals in the reaction chamber (methanol/methyl nitrite/NO/air) did not result in any of the data reported below except for small amounts (as noted by chromatographic peak areas) of acetone, 2-oxopropanal, and ethanedial. Acetone was also observed in pre-photoinitiated geraniol + OH or pre-ozonated geraniol + O_3 derivatization samples. However, the acetone, 2-oxopropanol, and ethanedial oxime peak areas increased significantly, between 30% and 70%, with geraniol + OH or geraniol + O_3 reaction initiation, indicating that acetone, 2-oxopropanal and ethanedial are likely products of the geraniol + OH and geraniol + O_3 reactions.

3.4. Acetone

Acetone was identified using the Agilent 6890/5973 GC/MS system and PFBHA derivatization method described above. The acetone oxime (PFBHA = $C(CH_3)_2$) was observed at approximately 7.6 min employing the Varian 3800/Saturn 2000 GC/ion trap mass spectrometer system described above. Acetone oxime was synthesized to confirm this chromatographic assignment. Acetone oxime was observed in pre-photolysis samples, but the peak area increased upon initiation of geraniol + OH reaction indicating acetone as a geraniol + OH reaction product. Acetone was also identified as a geraniol + O_3 reaction product.

3.5. Hydroxyacetaldehyde (glycolaldehyde, $CH(=O)CH_2OH$)

The chromatographic peaks for the oxime observed at 10.2 and 10.5 min were observed as a reaction product of geraniol + OH and had ions at m/z (relative intensity) 181 (100%), 195 (16%), 226 (11–24%), and 238 (45%). Using acetonitrile for chemical ionization, an $M+1$ ion of m/z of 256 was observed for the PFBHA-derivatized sample. The glycolaldehyde oxime was synthesized by heating the glycolaldehyde dimer in the gas phase (Magneron et al., 2005) to confirm this chromatographic assignment. This carbonyl compound was also observed as a geraniol + O_3 reaction product.

3.6. Ethanedial (Glyoxal, $HC(=O)C(1=O)H$)

The chromatographic peaks for the oxime observed at 24.9 and 25.2 min were observed as a reaction product of geraniol + OH and had ions at m/z (relative intensity) 181 (100%) and 448 (25%). The m/z 448 ion is the result of a double PFBHA derivatization indicating a reaction product with a molecular weight of 58. Using acetonitrile for chemical ionization, an $M+1$ ion of m/z of 449 was observed for the PFBHA-derivatized sample. The PFBHA-glyoxal oxime was synthesized to confirm this chromatographic assignment (Yu et al., 1998). This carbonyl compound was also observed as a geraniol + O_3 reaction product.

3.7. 2-Oxopropanal (Methylglyoxal, $CH_3C(=O)C(=O)H$)

The single peak for the oxime observed at 26.1 min was observed as a reaction product of geraniol + OH and had ions at m/z (relative intensity) 181 (100%) and 265 (31%). The m/z 462 ion is the result of a double PFBHA derivatization indicating a reaction product with a molecular weight of 72. Using acetonitrile for chemical ionization, an $M+1$ ion of m/z of 463 was observed for the PFBHA-derivatized sample. The PFBHA-methylglyoxal oxime was synthesized to confirm this chromatographic assignment (Yu et al., 1998). The second chromatographic peak for PFBHA-methylglyoxal overlaps with the 25.2 min peak of PFBHA-glyoxal. This carbonyl compound was also observed as a geraniol + O_3 reaction product.

3.8. Oxime at retention time 30.0, 30.3 and 30.7 min

The oxime observed with a chromatographic peak at a retention time of 30.0, 30.3 and 30.7 min had ions of m/z (relative intensity) 82 (16–23%), 181 (65–100%), 262 (15–20%), 263 (17–22%), 278 (34–51%), 279 (76–100%), and 490 (11–17%) as seen in Fig. 3A. The m/z 490 ion is the result of a double PFBHA derivatization indicating a reaction product with a molecular weight of 100. Using acetonitrile for chemical ionization, an $M+1$ ion of m/z of 491 was observed for the PFBHA-derivatized sample as seen in Fig. 3B. A proposed geraniol + OH reaction product assignment of 4-oxopentanal (see Table 1) was made based upon the observed data. This carbonyl compound was also observed as a geraniol + O_3 reaction product.

4. Discussion

OH reacts with geraniol by H-atom abstraction or OH addition to the carbon–carbon double bonds (Atkinson, 1989; Atkinson and Aschmann, 1993). The "reactive structure" of geraniol can be drawn as shown in Structure 1. The sites labeled I and II identified in Structure 1 contribute approximately 97%, to the calculated geraniol + OH rate constant of 180×10^{-12} cm^3 molecule^{-1} s^{-1} (US Environmental Protection Agency, 2000) which is slower than the measured value reported here $(231 \pm 58) \times 10^{-12}$ cm^3 molecule^{-1} s^{-1}.

Ozone reacts with geraniol by addition to the carbon–carbon double bond (sites I and II, Structure 1). The measured value reported here $(9.3 \pm 2.3) \times 10^{-16}$ cm^3 molecule^{-1} s^{-1} can be compared to both the calculated geraniol + O_3 rate constant using Environmental Protection Agency's rate constant calculation software, AOPWIN v1.91 is 8.6×10^{-16} cm^3 molecule^{-1} s^{-1} (US Environmental Protection Agency, 2000) and the calculated rate constant $\sim 4 \times 10^{-16}$ cm^3 molecule^{-1} s^{-1} from data of by Nunes et al. (Nunes et al., 2005).

For the geraniol + OH reaction the experimental parameters were set to minimize side reactions and highlight the primary OH hydrogen abstraction and OH addition step. The geraniol concentration was kept low and the photolysis times were as short as possible. Additionally, nitric oxide (NO) was added to facilitate the generation of OH and to minimize O_3 and NO_3 radical formation preventing other possible radical reactions. The possible mechanistic

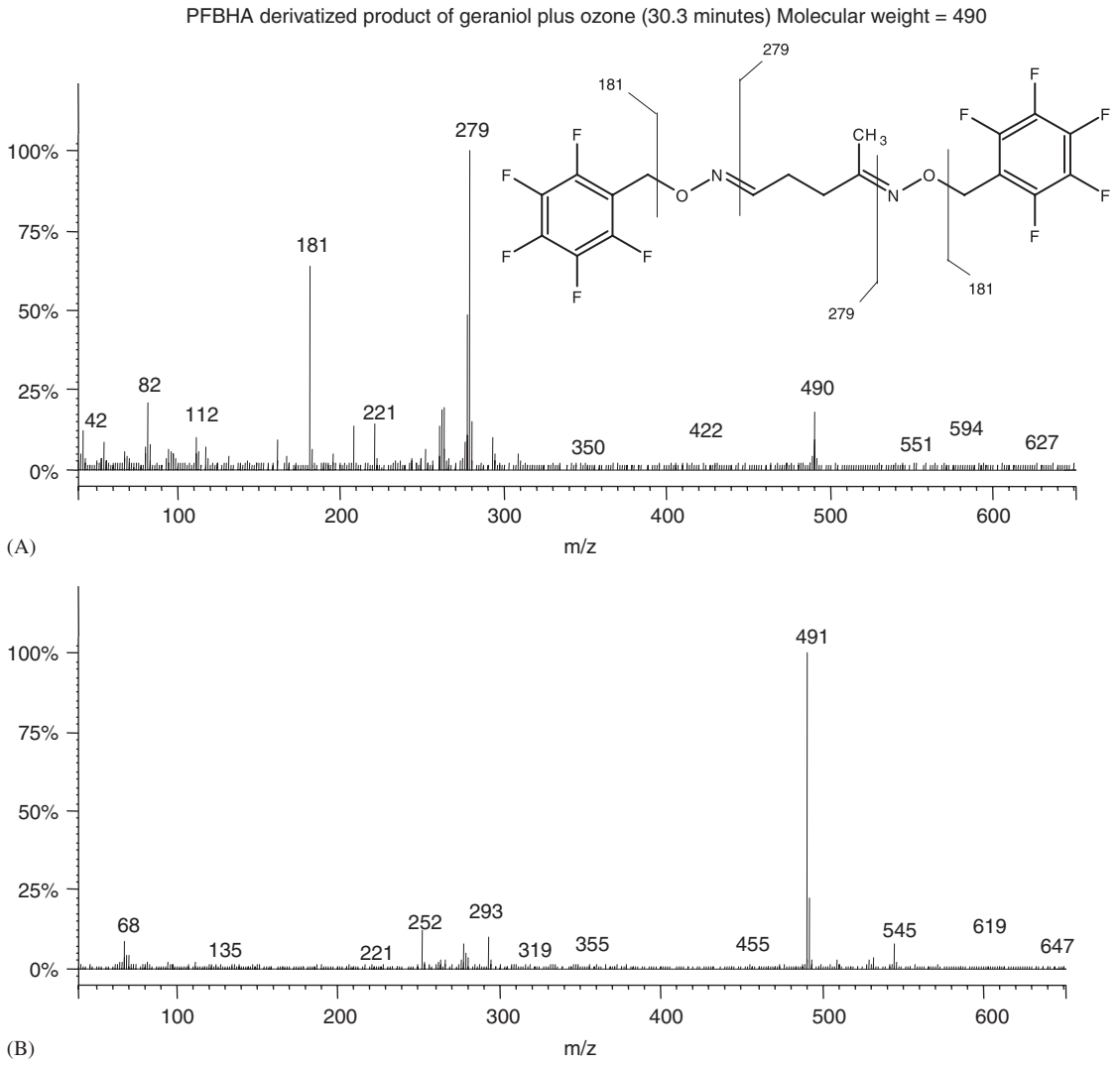

Fig. 3. PFBHA derivatized product of geraniol (30.3 min) (A) electron ionization spectrum (B) acetonitrile chemical ionization spectrum.

steps leading to product formation are described below.

4.1. Acetone

The geraniol + OH reaction mechanism has several potential pathways leading to acetone ($O{=}C(CH_3)_2$) formation. OH can react with geraniol by addition to site I to carbon (C3), producing the radical, $(CH_3)_2C(\cdot)CH(OH)CH_2CH_2C(CH_3){=}CHCH_2OH$. Subsequent addition of oxygen to the radical leads to decomposition and formation of the peroxyradical, $(CH_3)_2COO\cdot$ and the radical $OHC(\cdot)CHCH_2CH_2C{=}(CH_3)CHCH_2OH$. The $(CH_3)_2COO\cdot$ radical can then react with NO to form NO_2 and acetone. Acetone product formation from the geraniol + O_3 reaction has a similar mechanistic pathway to that of the geraniol + OH reaction.

4.2. Hydroxyacetaldehyde (glycolaldehyde)

OH can react with geraniol by addition to site II to carbon (C6), producing the radical $(CH_3)_2C{=}CHCH_2CH_2C(CH_3)(OH)CH(\cdot)CH_2OH$. Subsequent addition of oxygen to the radical leads to decomposition and formation of the peroxyradical, $CH_2(OH)CHOO\cdot$ and the radical $(CH_3)_2C{=}CHCH_2CH_2C(CH_3)(OH)(\cdot)$. The $CH_2(OH)CHOO\cdot$ radical can then react with NO to form

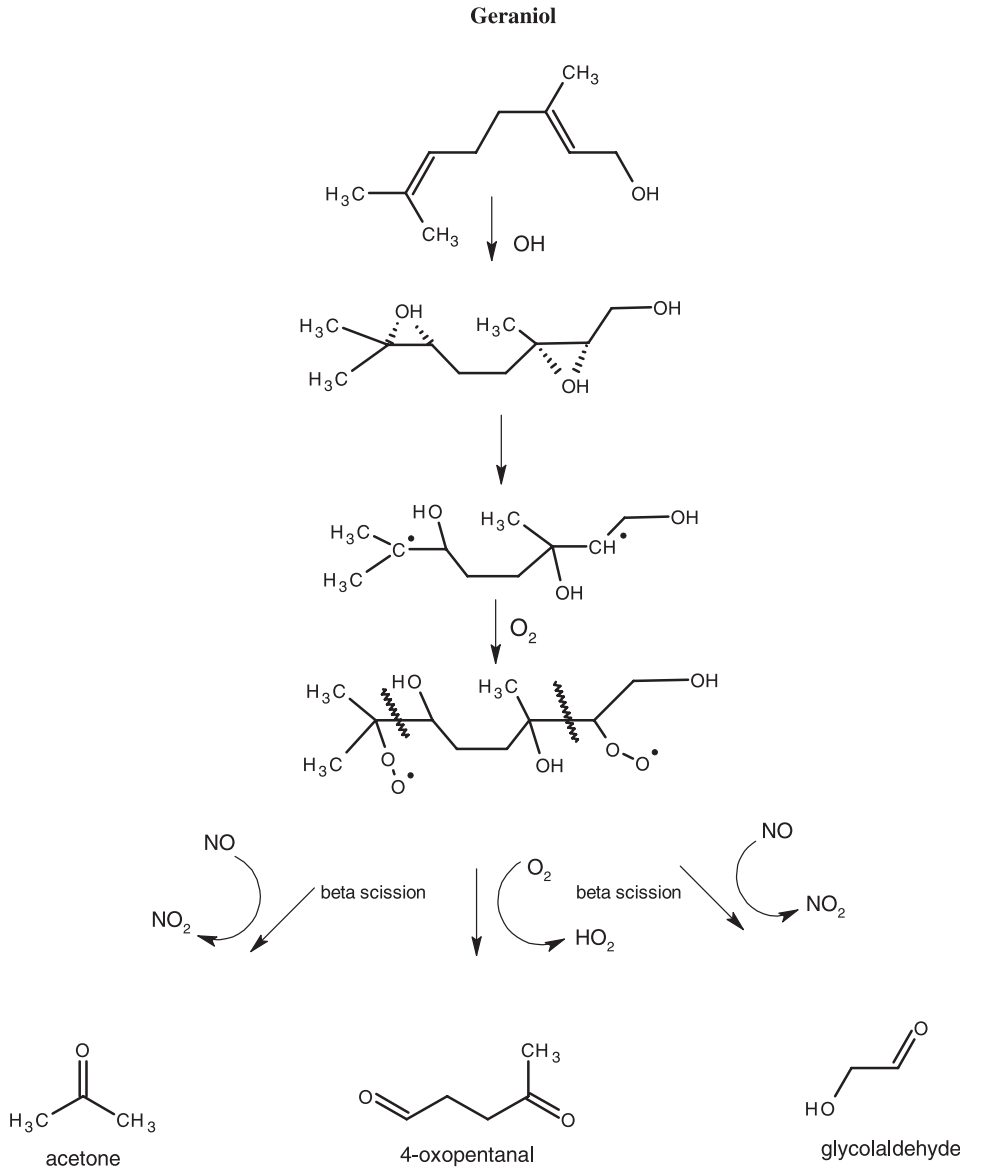

Fig. 4. Proposed reaction mechanism for geraniol + OH showing formation of acetone, glycolaldehyde and 4-oxopentanal.

NO_2 and glycolaldehyde. Glycolaldehyde product formation from the geraniol + O_3 reaction is similar to that of the geraniol + OH reaction.

4.3. 4-oxopentanal

The chromatographic peak proposed to be 4-oxopentanal based on mass spectral data was the largest product peak observed in the PFBHA derivatization experiments from the geraniol + OH and geraniol + O_3 reactions (Fig. 3). In the geraniol + OH reaction, 4-oxopentanal is likely formed from OH addition to sites I and II, as seen in Fig. 4. OH can add to either side of the double bond. If OH adds to both double bonds as described above resulting in acetone and glycolaldehyde, the resulting product is the radical $OHC(\cdot)CHCH_2CH_2C(\cdot)(CH_3)(OH)$. This radical reacts with O_2 to form HO_2 and 4-oxopentanal $O{=}CHCH_2CH_2C(CH_3){=}O$. 4-oxopentanal product formation from the geraniol + O_3 reaction is expected to be similar to that of the geraniol + OH reaction.

The reaction products: acetone, hydroxyacetaldehyde, ethanedial, 2-oxopropanal, and 4-oxopentanal appear in both the geraniol + OH and the geraniol + O_3 reactions. Ozone/alkene reactions can produce steady state OH radical concentrations which would explain the observation of these products in both reactions (Paulson et al., 1999). However, addition of a large concentration of cyclohexane (297 ppm) to scavenge OH radicals in the geraniol + O_3 reaction mixture effectively eliminates the geraniol + OH side reaction.

In a recent paper (Nunes et al., 2005), the authors specifically noted the absence of 4-oxopentanal as a reaction product of geraniol and ozone. Fig. 3 shows a mass spectrum of a PFBHA derivatized product of geraniol believed to be 4-oxopentanal. Also in the same paper, the authors listed cyclohexanone as a geraniol + O_3 reaction product. Cyclohexanone was also observed in this study, however, a more likely explanation of its presence is not as a geraniol + O_3 reaction product but as a result of the addition of cyclohexane as an OH radical scavenger (Paulson et al., 1999).

5. Conclusions

In order to investigate the detailed gas-phase chemistry of 2,6-dimethyl-2,6-octadien-8-ol (geraniol, Structure 1), the hydroxyl (OH) radical reaction rate constant, ozone reaction rate constant and respective reaction mechanisms were investigated. The OH radical can either abstract hydrogen or add to the carbon–carbon double bond of geraniol. A bimolecular rate constant, $k_{OH+geraniol}$, of $(231 \pm 58) \times 10^{-12}\,cm^3\,molecule^{-1}\,s^{-1}$ was measured using the relative rate technique. Ozone is expected to add to the carbon–carbon double bond of geraniol and a geraniol + O_3 rate constant, $k_{O_3+geraniol}$, of $(9.3 \pm 2.3) \times 10^{-16}\,cm^3\,molecule^{-1}\,s^{-1}$ was measured.

The identification of the geraniol + OH and geraniol + O_3 reaction products was facilitated by the use of derivatizing agents PFBHA and BSTFA. While many geraniol + OH reaction products were proposed based on previously published VOC/OH reaction mechanisms, reaction products such as acetone, hydroxyacetaldehyde, ethanedial, and 2-oxopropanal were positively identified using the observed experimental data. The major reaction product, 4-oxopentanal, was proposed based on mass spectral data from the PFBHA and BSTFA experiments and published mechanisms. The structures of the identified reaction products indicate that the carbon–carbon double bonds (geraniol + O_3 and geraniol + OH) play important roles in the formation of reaction products.

Approximate indoor environment concentrations of the hydroxyl radical (1.23×10^5 molecules cm^{-3}) and ozone (4.92×10^{11} molecules cm^{-3}) have been previously estimated by Sarwar (Sarwar et al., 2002). Using the geraniol + OH and geraniol + O_3 rate constants reported here pseudo-first order rate constants of 0.10 and 1.64 h^{-1} were determined, respectively. Comparing these values to a typical indoor air exchange rate of 0.6 h^{-1}, the geraniol + O_3 reaction is expected to be the most likely indoor environment loss mechanism for geraniol (Wilson et al., 1996).

Disclaimer. The findings and conclusions in this report are those of the authors and do not necessarily represent the views of the National Institute for Occupational Safety and Health.

References

Atkinson, R., 1989. Kinetics and mechanisms of the gas-phase reactions of the hydroxyl radical with organic compounds. Journal of Physical Chemical Reference Data, Monograph 1, 246.

Atkinson, R., 1994. Gas-phase tropospheric chemistry of organic compounds. Journal of Physical Chemical Reference Data, Monograph 2, 215.

Atkinson, R., 2003. Kinetics of the gas-phase reactions of OH radicals with alkanes and cycloalkanes. Atmospheric Chemistry and Physics Discusssions 3, 4183–4358.

Atkinson, R., Aschmann, S.M., 1993. OH radical production from the gas-phase reactions of O_3 with a series of alkenes under atmospheric conditions. Environmental Science & Technology 27, 1357–1363.

Atkinson, R., Carter, W.P.L., Winer, A.M., Pitts, J.N., 1981. An experimental protocol for the determination of OH radical rate constants with organics using methyl nitrite photolysis as an OH radical source. Journal of the Air Pollution Control Association 31, 1090–1092.

Boethling, R.S., Mackay, D., 2000. Handbook of Property Estimation Methods for Chemicals: Environmental and Health Sciences. Lewis Publishers, New York.

Bradley, W.R., Wyatt, S.E., Wells, J.R., Henley, M.V., Graziano, G.M., 2001. The hydroxyl radical reaction rate constant and products of cyclohexanol. International Journal of Chemical Kinetics 33, 108–117.

Dales, R., Raizenne, M., 2004. Residential Exposure to Volatile Organic Compounds and Asthma. J Asthma 41, 259–270.

Fick, J., Pommer, L., Nilsson, C., Andersson, B., 2003. Effect of OH radicals, relative humidity, and time on the composition of the products formed in the ozonolysis of alpha-pinene. Atmospheric Environment 37, 4087–4096.

Jarvis, J., Seed, M.J., Elton, R.A., Sawyer, L., Agius, R.M., 2005. Relationship between chemical structure and the occupational

asthma hazard of low molecular weight organic compounds. Occup Env Med 62, 243–250.

Magneron, I., Mellouki, A., Le Bras, G., Moortgat, G.K., Horowitz, A., Wirtz, K., 2005. Photolysis and OH-initiated oxidation of glycolaldehyde under atmospheric conditions. Journal of Physical Chemistry A 109, 4552–4561.

Nazaroff, W.W., Weschler, C.J., 2004. Cleaning products and air fresheners: exposure to primary and secondary air pollutants. Atmospheric Environment 38, 2841–2865.

NIOSH, 2004. Chapter 2: Respiratory Diseases. Worker Health Chartbook. Publication No. 2004-146.

Nunes, F.M.N., Veloso, M.C.C., Pereira, P., de Andrade, J.B., 2005. Gas-phase ozonolysis of the monoterpenoids (S)-(+)-carvone, (R)-(−)-carvone, (−)-carveol, geraniol and citral. Atmospheric Environment 39, 7715–7730.

Orji, L.N., Stone, D.A., 1992. Relative rate-constant measurements for the gas-phase reactions of hydroxyl radicals with 4-methyl-2-pentanone, trans-4-octene, and trans-2-heptene. International Journal of Chemical Kinetics 24, 703–710.

Paulson, S., Chung, M.Y., Hasson, A.S., 1999. OH radical formation from the gas-phase reaction of ozone with terminal alkenes and the relationship between structure and mechanism. Journal of Physical Chemistry A 103, 8125–8138.

Sarwar, G., Corsi, R., Kimura, Y., Allen, D., Weschler, C.J., 2002. Hydroxyl radicals in indoor environments. Atmospheric Environment 36, 3973–3988.

Sexton, K.G., Jefferies, H.E., Jang, M., Kamens, R.M., Doyle, M., Voicu, I., Jaspers, I., 2004. Photochemical products in urban mixtures enhance inflammatory responses in lung cells. Inhalation Toxicolology 16, 107–114.

Smith, D.F., Kleindienst, T.E., Hudgens, E.E., McIver, C.D., Bufalini, J.J., 1992. Kinetics and mechanism of the atmospheric oxidation of ethyl tertiary butyl ether. International Journal of Chemical Kinetics 24, 199–215.

Smith, D.F., McIver, C.D., Kleindienst, T.E., 1995. Kinetics and mechanism of the atmospheric oxidation of tertiary amyl methyl-ether. International Journal of Chemical Kinetics 27, 453–472.

Taylor, W.D., Allston, T.D., Moscato, M.J., Fazekas, G.B., Kozlowski, R., Takacs, G.A., 1980. Atmospheric photodissociation lifetimes for nitromethane, methyl nitrite, and methyl nitrate. International Journal of Chemical Kinetics 12, 231–240.

US Environmental Protection Agency, 2000. AOPWIN v1.91. Washington D.C., 〈http://www.epa.gov/opptintr/exposure/docs/episuite.htm〉, (accessed: 14 February 2005).

Veillerot, M., Foster, P., Guillermo, R., Galloo, J.C., 1996. Gas-phase reaction of n-butyl acetate with the hydroxyl radical under simulated tropospheric conditions: relative rate constant and product study. International Journal of Chemical Kinetics 28, 235–243.

Wallington, T.J., Andino, J.M., Potts, A.R., Rudy, S.J., Siegl, W.O., Zhang, Z.Y., Kurylo, M.J., Hule, R.E., 1993. Atmospheric chemistry of automotive fuel additives—diisopropyl ether. Environmental Science & Technology 27, 98–104.

Weisel, C.P., 2002. Assessing exposure to air toxics relative to asthma. Env Health Perspec 110, 527–537.

Wells, J.R., 2004. The hydroxyl radical reaction rate constant and products of 3,5-dimethyl-1-hexyn-3-ol. International Journal of Chemical Kinetics 36, 534–544.

Wells, J.R., 2005. Gas-phase chemistry of alpha-terpineol with ozone and OH radical: rate constants and products. Environmental Science & Technology 39, 6937–6943.

Wells, J.R., Wiseman, F.L., Williams, D.C., Baxley, J.S., Smith, D.F., 1996. The products of the reaction of the hydroxyl radical with 2-ethoxyethyl acetate. International Journal of Chemical Kinetics 28, 475–480.

Weschler, C.J., 2001. Reactions among indoor pollutants. Journal of the Scientific World 1, 443–457.

Weschler, C.J., Shields, H.C., 1996. Production of the hydroxyl radical in indoor air. Environmental Science & Technology 30, 3250–3258.

Weschler, C.J., Shields, H.C., 1997a. Measurements of the hydroxyl radical in a manipulated but realistic indoor environment. Environmental Science & Technology 31, 3719–3722.

Weschler, C.J., Shields, H.C., 1997b. Potential reactions among indoor pollutants. Atmospheric Environment 31, 3487–3495.

Wieslander, G., Norback, D., Bjornsson, E., Janson, C., Boman, G., 1997. Asthma and the indoor environment: the significance of emission of formaldehyde and volatile organic compounds from newly painted indoor surfaces. Int Arch Occup Environ Health 69, 115–124.

Williams, D.C., Orji, L.N., Stone, D.A., 1993. Kinetics of the reactions of OH radicals with selected acetates and other esters under simulated atmospheric conditions. International Journal of Chemical Kinetics 25, 539–548.

Wilson, A.L., Colome, S.D., Tian, Y., Becker, E.W., Baker, P.E., Behrens, D.W., Billick, I.H., Garrison, C.A., 1996. California residential air exchange rates and residence volumes. Journal of Exposure Analysis and Environmental Epidemiology 6, 311–326.

Wyatt, S.E., Baxley, S., Wells, J.R., 1999. The hydroxyl radical reaction rate constant and products of methyl isobutyrate. International Journal of Chemical Kinetics 31, 551–557.

Yu, J.Z., Flagan, R.C., Seinfeld, J.H., 1998. Identification of products containing –COOH, –OH, and –C═O in atmospheric oxidation of hydrocarbons. Environmental Science & Technology 32, 2357–2370.

Zhang, J., Smith, K.R., 2003. Indoor air pollution: a global health concern. Brit Med Bull 68, 209–225.